


## Article

# Technogenic Reservoirs Resources of Mine Methane When Implementing the Circular Waste Management Concept

Vladimir Brigida <sup>1,2,\*</sup> , Vladimir Ivanovich Golik <sup>3</sup>, Elena V. Voitovich <sup>4</sup>, Vladislav V. Kukartsev <sup>5,6,7</sup>, Valeriy E. Gozbenko <sup>8,9</sup>, Vladimir Yu. Konyukhov <sup>10</sup> and Tatiana A. Oparina <sup>10</sup>

- <sup>1</sup> Laboratory of Mining Technical Systems Management, Research Institute of Comprehensive Exploitation of Mineral Resources of the Russian Academy of Sciences, 4 Kryukovskiy Tupik, 111020 Moscow, Russia
  - <sup>2</sup> Department of Biomedical, Veterinary and Ecological Directions, RUDN University, 117198 Moscow, Russia
  - <sup>3</sup> Department “Technique and Technology of Mining and Oil and Gas Production”, Moscow Polytechnic University, 33 B. Semenovskaya St., 107023 Moscow, Russia; v.i.golik@mail.ru
  - <sup>4</sup> Department of Industrial and Civil Engineering, Moscow Polytechnic University, 107023 Moscow, Russia
  - <sup>5</sup> Department of Informatics, Institute of Space and Information Technologies, Siberian Federal University, 660041 Krasnoyarsk, Russia
  - <sup>6</sup> Department of Information Economic Systems, Institute of Engineering and Economics, Reshetnev Siberian State University of Science and Technology, 660037 Krasnoyarsk, Russia
  - <sup>7</sup> Artificial Intelligence Technology Scientific and Education Center, Bauman Moscow State Technical University, 105005 Moscow, Russia
  - <sup>8</sup> Department of Organization of Transportation and Management on Motor Transport, Angarsk State Technical University, 665835 Angarsk, Russia
  - <sup>9</sup> Department of Mathematics, Irkutsk State Transport University, 664074 Irkutsk, Russia
  - <sup>10</sup> Department of Automation and Control, Irkutsk National Research Technical University, 664074 Irkutsk, Russia
- \* Correspondence: 1z011@inbox.ru



**Citation:** Brigida, V.; Golik, V.I.; Voitovich, E.V.; Kukartsev, V.V.; Gozbenko, V.E.; Konyukhov, V.Y.; Oparina, T.A. Technogenic Reservoirs Resources of Mine Methane When Implementing the Circular Waste Management Concept. *Resources* **2024**, *13*, 33. <https://doi.org/10.3390/resources13020033>

Academic Editors: Carlo Ingrao, Alberto Bezama, Annarita Paiano, Jakob Hildebrandt and Claudia Arcidiacono

Received: 9 December 2023

Revised: 27 January 2024

Accepted: 5 February 2024

Published: 17 February 2024



**Copyright:** © 2024 by the authors. Licensee MDPI, Basel, Switzerland. This article is an open access article distributed under the terms and conditions of the Creative Commons Attribution (CC BY) license (<https://creativecommons.org/licenses/by/4.0/>).

**Abstract:** From a commercial viewpoint, mine methane is the most promising object in the field of reducing emissions of climate-active gases due to circular waste management. Therefore, the task of this research is to estimate the technogenic reservoirs resources of mine methane when implementing the circular waste management concept. The novelty of the authors’ approach lies in reconstructing the response space for the dynamics of methane release from the front and cross projections:  $CH_4 = f(S; t)$  and  $CH_4 = f(S; L)$ , respectively. The research established a polynomial dependence of nonlinear changes in methane concentrations in the mixture extracted by type 4 wells when a massif is undermined as a result of mining in a full-retreat panel. And the distance from the face to the start of mining the panel is reduced by 220 m. For this reason, the emission of mine methane, in case of degasification network disruption in 15 days, can amount to more than 660 thousand m<sup>3</sup> only for wells of type no. 4.

**Keywords:** mine methane; resource recovery; circular waste management; sustainability; gas flow

## 1. Introduction

Global methane emissions (containing a mine methane proportion in the range of 11–13% [1]) can account for up to 19% of the total emissions of climatically active gases [2]. At the same time, our country’s share in its global emissions, according to rough estimates obtained from foreign sources, amounted to about 7%, 50% of which was due to mining [3]. Estimating indirect gas emissions is difficult, even when using modern methods. This is related to the problems of modeling the process of drainage from technogenic methane reservoirs in dead pits or previously abandoned sublevels of operating mining enterprises. This fact makes it particularly necessary to switch to sustainable geotechnologies [4–8]. The transition to sustainable development is a necessary measure to mitigate the consequences of global climate change [9–11]. The main measures are considered to be the

following. The first is increasing the share of renewable energy sources. The second is improving the system of monitoring the pollutants [12]. The third is the introduction of low-carbon technologies, including the formation of cadasters and technologies that reduce greenhouse gas emissions [13,14]. The fourth is digitalization of the power and extractive industries, and increasing the energy efficiency of production processes [15–17] involved in the development and implementation of negative emission technologies [18]. In addition, one of the dynamically developing areas in recent years is the introduction of closed-loop economy elements when improving mining and metallurgical production (when the resources circulate without the “end of life cycle” [19–21]). Much attention is paid to this area in EU countries. This study indicates that a set of closed-loop economic measures can increase the EU’s GDP by 1% by 2030, resulting in 2 million additional jobs. In England, measures to promote the “circular economy” [22,23] are expected to contribute to attracting EUR 12 billion of investments and creating 50 thousand new jobs [24]. This is gradually coming to the forefront in such countries as China [25–27]. To achieve carbon neutrality by 2060, most authoritative scientists propose introducing a tax on coal resources, which, on the one hand, can lead to an increase in prices for coal products and, on the other hand, is an effective way to reduce coal consumption [25]. One of the relatively new ways to achieve sustainable development based on the greening of mining production is cyclical economy elements, the so-called cyclical waste management (CWM) [28–30].

Implementing the circular waste management concept for mine methane (converting waste into energy [30]) implies the need to improve the quality and volume of gas extraction from technogenic reservoirs, and to generate electricity for its connection to the mine’s energy system (with the introduction of cogeneration technologies [31]). The relevance of such studies can hardly be overestimated, and the evidence of the relationship between increasing the efficiency of underground degassing and reducing technogenic emission processes (caused by extracting the subsurface minerals) still remains insufficiently studied.

The methane distribution in the mined-out space of coal mines and in rock massifs has been studied in many works [32], while the main focus has shifted to analytical and instrumental methods [33]. Study [34] states that a breakthrough is currently required to predict methane emissions (due to the limitation of the traditional approaches).

One of the most controversial issues is forecasting zones with different filtration channel parameters of the “methane drainage zone” in a disintegrating metastable solid coal–gas solution, and their boundaries (angles of complete shifts) [35–37] for real conditions of reserves mining. The issues of describing the peculiarities of aerogas processes caused by stopping have been explored quite fully, and were discussed in [38]. The metal release dynamics, in turn, are subject to a number of mining factors whose cumulative effect is quite difficult to describe. In a number of domestic scientific research studies [39–42], attempts were made to model the distribution of methane fluxes. In some works [43–45], the authors consider a three-dimensional formulation of the problem. The numerical methods that have proven themselves well when considering specific aspects [46,47] cannot always be successfully applied when dealing with three-dimensional models. At the same time, the issues of losing a part of the methane resources obtained from the technogenically disturbed massif, owing to the low efficiency of degassing the mined-out space, have not been fully studied. In this regard, it follows that the issues of identifying the peculiarities of the migration of coal mine methane flows into the mined-out space cavity of longwalls abandoned earlier (accompanied by a subsequent release into the atmosphere), as well as approaches to their modeling, need to be improved. The scientific idea of the project is using the regularities of the influence of the spatial-temporal development of the stoping to determine the nonlinear component of the aerogas mode of the undermined degassing wells. Analysis of the current state of the issue in the area under consideration allows for the conclusion that the closest research direction is substantiating the parameters of the three-dimensional spatial orientation of wells for degassing the undermining coal rock mass. The well-known formulation of the problem does not take into account the peculiarities of the nonlinear nature of methane release dynamics (the fourth dimension is  $t$ ), as well as the

technogenic disturbance intensity during the spatial-temporal development of the stoping as a result of mining deep-lying high-gas coalbeds. The conditions of this problem reveal the fact that at the first stage, it is necessary to reduce the number of space measurements to one (in our case, this is “S, m” denoting the distance to the start of the full-retreat panel). The following difficult moment (not fully resolved) is associated with the mechanism of the impact of the bottom movement on the “space-time” system of a longwall, which is different from the “space-time” system of the state of each well (or a static system of the degassing network elements). At this stage, a hypothesis was considered for the partial stabilization of the longwall influence on the methane concentration dynamics “CH<sub>4</sub>, %” through the parameter “L, m” (the distance from the head of each well to the longwall face at each moment of time).

In view of this, for the first time during a limited consideration of a four-dimensional spatial-temporal task (i.e., without L in the CH<sub>4</sub>-t plane), according to the planned approach, the parameter S was introduced. This allows consideration of the process under study as a (prescribed implicitly) CH<sub>4</sub> function of S (the space axis being a distance from the beginning of the site “by the analogy with the distance from the beginning of the site to the longwall position at other times”)-t (measurement time). The next important aspect remaining is to obtain a theoretical model [48,49] (a process formula or regression having a specified goodness-of-fit level), which is still an open fundamental scientific problem in the case of three-dimensional models (see, for instance, [50,51]).

In this regard, developing measures (based on the methane concentration dynamics in mixtures extracted by underground boreholes on operating mines) aimed at preventing the loss of energy resources based on new regularities of the spatial-temporal variability of gas flows is an urgent scientific task. The purpose of this research is to estimate technogenic reservoirs resources of mine methane when implementing the circular waste management concept.

## 2. Materials and Methods

**Object.** The object of the study is a degassable massif during mining the m<sup>3</sup> reservoir, implemented at the AP “Minen.a. A.F. Zasyadko”, which is located in the central part of the Donetsk-Makeyevsky geological and industrial district in the territory of Donetsk city. The Shakhtnoye site borders the Oktyabrsky mine in the west and the K. I. Pochenkov mine in the east. Downdip, the minefield borders the abandoned sublevel of the Kalmius mine. It was designed by the “Yuzhgiproshakht” Institute in 1948 and commissioned in 1958. The design capacity of the mine is 1.2 million tons of coal. After the introduction of a new horizon, the mine’s capacity reached 1.8 million tons. The abundance of the methane released from the working areas, when developing m<sup>3</sup> and l1 beds, reaches 90 m<sup>3</sup>/min. Ensuring the gas safety of the mining requires capturing and bringing to the surface at least 70 m<sup>3</sup>/min of methane (200 m<sup>3</sup>/min of the gas mixture) from each area. The aggregate bed thickness is 1.37–1.76 m, with an average thickness of 1.53 m. The dip angle is 4–8°. The volume weight of the coal in the massif is 1.33 t/m<sup>3</sup>. The ash content is 8.3–12%, the humidity is 1–1.21%, the sulfur content is 3.86, the volatile yield is 32.3–33.6%, and the natural gas content ranges from 22 to 24 m<sup>3</sup>/ton of the dry ash-free mass. The bed is dangerous due to spontaneous combustion, coal and gas emissions, bleedings, and coal dust explosions. The bench is not dangerous in terms of sudden methane breakouts proceeding from the bottom.

The immediate mine roof over the entire area of the mine section is represented by argillite, which is also the main roof that is 10.45–16.3 m in thickness. As far as the stability is concerned, argillite is classified as low-resistant (B3), and in the places where weak adhesion is present, the stratification is unstable (B2). In the areas bearing pressure and tectonic disturbances, it is very unstable (B1). The collapse categories of the immediate and main roofs are A1, A2, and A3. The main bottom of the bed is of medium-stability siltstone (P2) whose thickness is 3.95–8.2 m.

A map extract of the plan of mining the m<sup>3</sup> bed is shown in Figure 1.

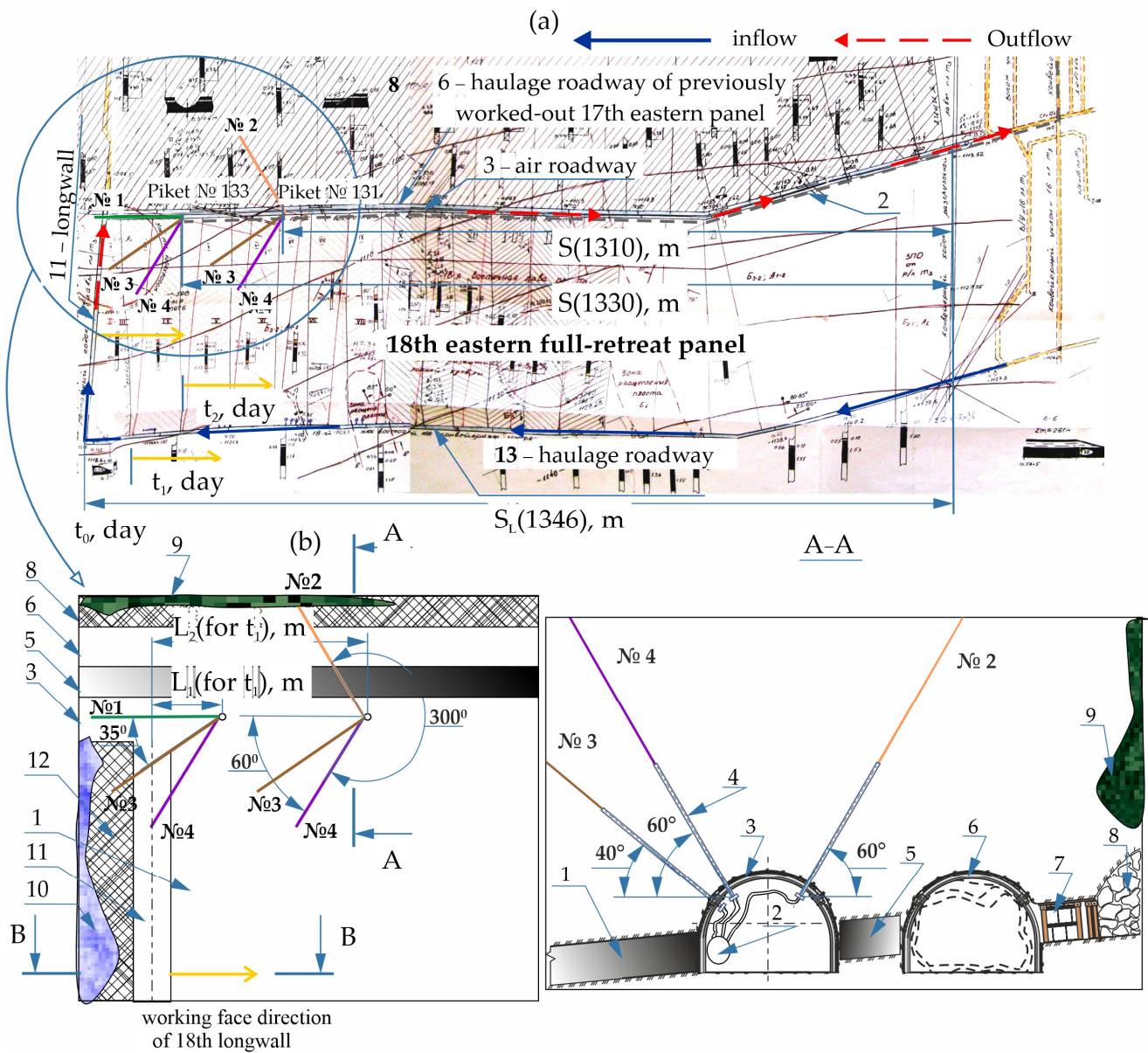


**Figure 1.** Mountain-geological conditions of the 18th eastern longwall mine on a seam  $m_3$ : (a)—top view, a plan of mining operations along seam  $m_3$  and stages of panel development ( $t_1$   $t_2$ , ...); (b)—schematic representation of wells (with inclination angles  $\beta$ ) drilled at the 133rd and 13st pickets; A–A—section drawn perpendicular to the roadway and parallel to the face (with boreholes azimuths  $\varphi$ ); B–B—section made perpendicular to the face; No. 1, 2, 3, 4—methane drainage boreholes; 1—seam  $m_3$ ; 2—degasification pipeline; 3—air roadway of the 18th eastern panel; 4—casing; 5—coal pillar; 6—haulage air roadway of the 17th eastern panel (which has been fully worked out up to this time); 7—auxiliary construction to protect the roadway; 8—mined-out space (goaf); 9—technogenic reservoirs of a mine methane in seam under a working zone of the previously mined panel of the 17th eastern longwall; 10—technogenic reservoirs of mine methane in the mined-out space and a seam under a working zone of the seam  $m_3$ ; 11—18th longwall; 12—goaf 18th eastern longwall; 13—haulage roadway.

Up to eight simultaneously operating vacuum pumps, whose maximum feed was  $50 \text{ m}^3/\text{min}$ , were used to degass one longwall, discharging the gas–air mixture through a pipeline 625 mm in diameter. The drilling pattern in the guiding beds is shown in Figure 2.

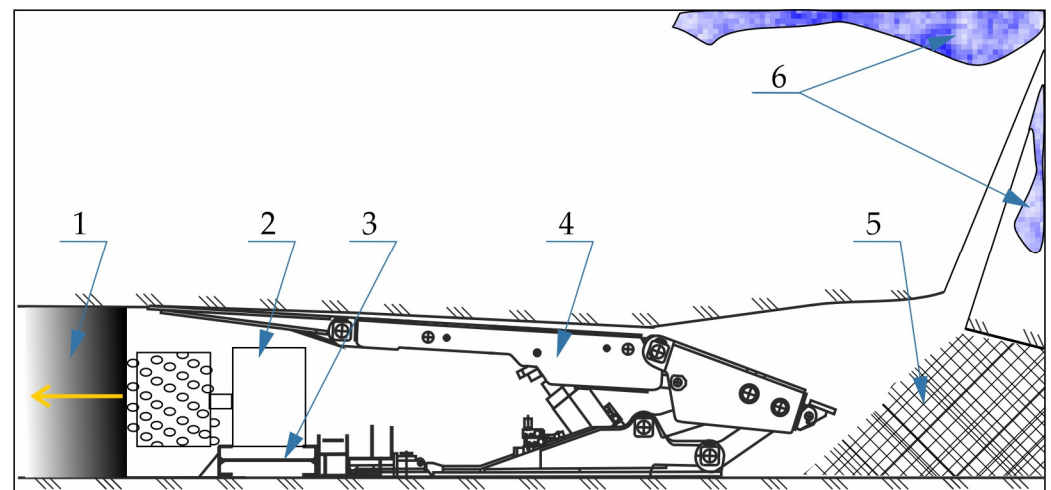


**Figure 2.** A section B–B indicated in Figure 1 made perpendicular to the working face: 1—coal seam  $m_3$ ; 2—schematic representation of a shearer loader with rows of teeth on the executive body; 3—flight conveyor; 4—section of a powered support in a longwall; 5—goaf 18th eastern longwall; 6—technogenic reservoirs of mine methane in a mined-out space and a seam under a working zone of the seam.

The initial data intended for constructing three-dimensional models were taken from [52]. The data are a set of measurements of the methane concentration on the 18th eastern longwall of the  $m^3$  bed conducted in the PAO “Zasyadko” obtained from [52].

**The measurements were carried out as follows.** Gas was collected from the wellhead of all operating boreholes at picket nos. 133, 131, 128, 126, 123, 121, 119, 117, 115, 113, and 111 in the first 6 months of panel operation. From the fitting placed at the wellhead of each well, samples of the gas–air mixture were taken into rubber chambers of standard sizes, after which the methane content in them was measured with gas analyzers. The mixture flow rate ( $Q$ ,  $m^3/min$ ) at each wellhead was determined (selectively, as it is closely related to the methane concentration in the mixture) using measuring diaphragms (a standard method). Monitoring was performed during the repair shift at the maximum frequency (pauses in measurement times did not exceed 4 days). The readings were taken in three repetitions using the Dräger X-AM 2500 c device (CatEx 125 PR mining is a stationary sensor with an error of  $\pm 2\%$ ) and duplicated on the SHI-12 (discrepancies did not exceed 15% and, in our opinion, they were conditioned by the high quality of the German instrument). A set of methane concentration measurements ( $CH_4$ ) obtained from each well made it possible to assess the nature of the distribution of gas flows throughout the entire local degassing network at each moment in time when the  $m^3$  formation was being mined.

**Objective.** In this case, the problem of determining the function of the methane concentration dynamics was considered, which is preset implicitly (in a specific example, the value of the gas concentration in the mixture extracted by underground degassing wells). Its change is influenced by the following factors. The first is the space in the form of a line along which the wells are drilled ( $S$ , m). It is conditionally identical to the distance from the beginning of the sublevel to each wellhead ( $Sp$ ). There is also the time of measuring ( $t$ , days), the influence factor of a longwall, which does not include the time of finding the face at the picket marks and the actual value of this picket ( $S_L$ ). This setting implies a 5-dimensional representation in view of the presence of the response function itself (methane concentration,  $CH_4$ ) and four factors =  $f(t_p; t_L; Sp; S_L)$ . If longwall position factors are replaced by the distance from it to the wellhead ( $L$ ), this problem can be reduced to two three-dimensional response spaces,  $CH_4 = f(t; S)$  and  $CH_4 = f(L; S)$ . As a result, a response space in the form of a set of the surfaces of the methane concentration dynamics in the extracted mixture ( $CH_4$ ) can be presented as  $f(S; t; L)$ . The novelty of the authors’ approach lies in restoring the response space from its front and cross projections. The

qualitative representation of the projections of two surfaces of the form  $CH_4 = f(S; t)$  and  $CH_4 = f(S; L)$  is the subject of further research.

In addition, the rational B-spline method was used to smooth out noise that is present in the data. In contrast to machine learning methods or Bayesian classification models [53–56], deterministic models were used. The obtained response surfaces were visualized in “gnuplot” software [57,58], analogously with [59].

### 3. Results

The data obtained from the previous studies [60,61] were presented in the form of a generalized regression model (Figure 3), in order to compare them with the options intended for creating two-dimensional models.

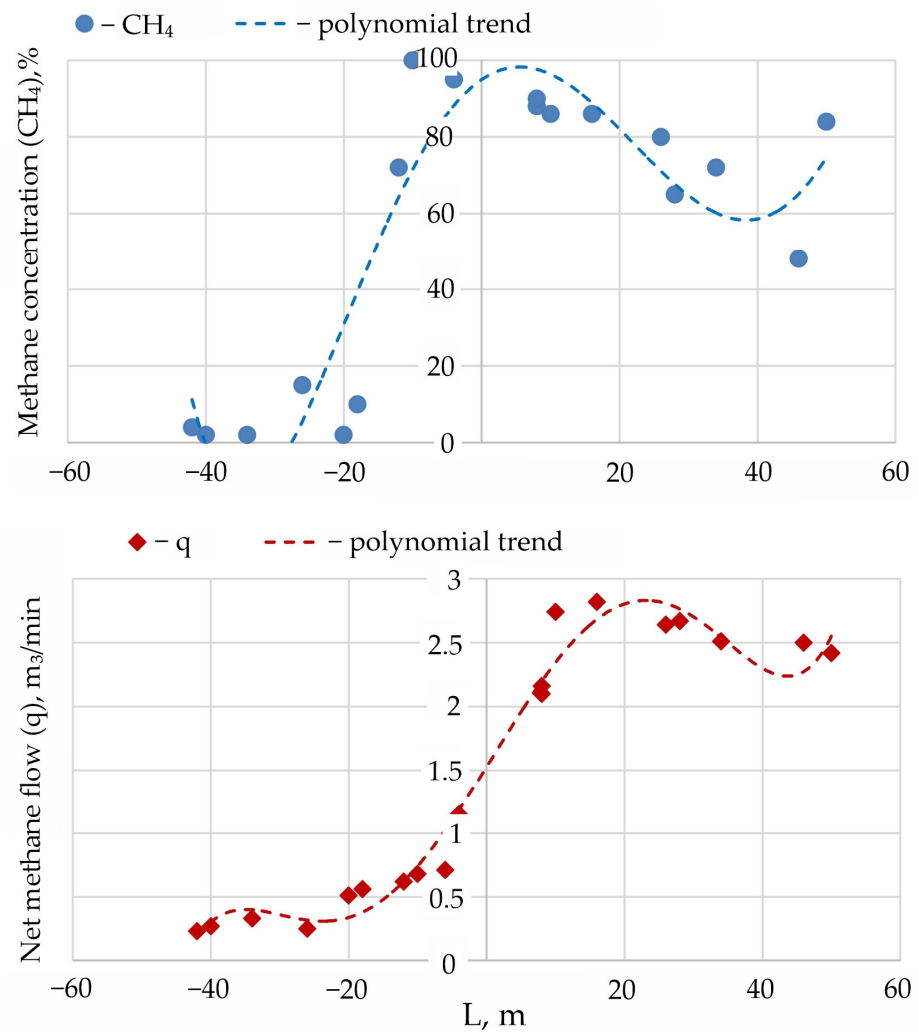


**Figure 3.** Dynamics of the methane concentration (%) and the net flow rate (methane flow,  $m^3/min$ ) depending on a face position in an undermined degassing well of type no. 4 (picket no. 133).

The analysis of the generalized trend line allows the conclusion that the methane release intensifies after the longwall passage, and can transit into an emission component due to the roof subsidence in the mined-out space. It is difficult to estimate the volume and the intensity of these processes.

The equation of the polynomial curve under study has the following form ( $R^2 = 0.846$ ):

$$CH_4 = -5E - 09L^6 - 3E - 07L^5 + 6E - 05L^4 + 0.0002L^3 - 0.1257L^2 + 1.2629L + 96.075 \tag{1}$$

In view of the complexity of considering multidimensional tasks, as well as improving the general methodology used for considering spatial-temporal geocological problems, wells of type number 4 (whose angle of elevation and turn = 60°) were selected for further research (devoted to using rational cubic, quadratic inhomogeneous B-splines).

In our case, the problem  $CH_4 = f(S; L)$  was solved based on [62]. The formula of the response surface has a polynomial form ( $S = S'$  for all  $S' \in [0, \pi]$  and  $L = L'$  for all  $L' \in [0, \pi]$ ):

$$\begin{aligned}
 CH_4 = & 68.3 - 6.6 \cos(S) + 12.5 \cos(L) + 15.2 \cos(2S) - 43.3 \cos(S) \cos(L) + 30.8 \cos(2L) - \\
 & 23.7 \cos(3S) + 21.7 \cos(2S) \cos(L) - 3.79 \cos(S) \cos(2L) - 12.59 \cos(3L) + 3.69 \cos(4S) - \\
 & 31.28 \cos(3S) \cos(L) + 17.4 \cos(2S) \cos(2L) - 14.2 \cos(S) \cos(3L) - 14.4 \cos(4L) - \\
 & 0.29 \cos(5S) + 10.8 \cos(4S) \cos(L) + 1.1 \cos(3S) \cos(2L) - 8.0 \cos(2S) \cos(3L) + \\
 & 10.5 \cos(S) \cos(4L) - 4.6 \cos(5L) + 4.06 \cos(6S) - 12.5 \cos(5S) \cos(L) - \\
 & 8.3 \cos(4S) \cos(2L) + 2.5 \cos(3S) \cos(3L) - 0.4 \cos(2S) \cos(4L) + 10.2 \cos(S) + \\
 & \cos(5L) - 0.8 \cos(6L) - 3.6 \cos(7S) + 6.6 \cos(6S) \cos(L) - 8.5 \cos(5S) \cos(2L) - \\
 & 8.5 \cos(4S) \cos(3L) + 1.2 \cos(3S) \cos(4L) - 0.5 \cos(2S) \cos(5L) + 3.5 \cos(S) \cos(6L) - \\
 & 3.8 \cos(7L) + 0.4 \cos(8S) - 5.8 \cos(7S) \cos(L) - 4.7 \cos(6S) \cos(2L) + \\
 & 6.9 \cos(5S) \cos(3L) + 7.1 \cos(4S) \cos(4L) - 6.4 \cos(3S) \cos(5L) + \\
 & 5.5 \cos(2S) \cos(6L) - 3.8 \cos(S) \cos(7L) - 3.4 \cos(8L) - 2.6 \cos(9S) + \\
 & 4.5 \cos(8S) \cos(L) - 1.2 \cos(7S) \cos(2L) - 0.2 \cos(6S) \cos(3L) + 4.4 \cos(5S) \cos(4L) - \\
 & 0.8 \cos(4S) \cos(5L) - 2.3 \cos(3S) \cos(6L) + 1.0 \cos(2S) \cos(7L) + 0.6 \cos(S) \cos(8L) - \\
 & 3.9 \cos(9L) + 1.1 \cos(10S) - 3.9 \cos(9S) \cos(L) - 0.6 \cos(8S) \cos(2L) + \\
 & 1.1 \cos(7S) \cos(3L) + 3.5 \cos(6S) \cos(4L) - 4.6 \cos(5S) \cos(5L) + \\
 & 1.6 \cos(4S) \cos(6L) + 1.3 \cos(3S) \cos(7L) + 1.3 \cos(2S) \cos(8L) + \cos(L) + \\
 & 3.1 \cos(S) \cos(9L) - 1.8 \cos(10L).
 \end{aligned} \tag{2}$$

One of the disadvantages of the above Equation (1) is neglecting the time factor, which is an objective difficulty in considering four-dimensional problems. In view of this, in a three-dimensional formulation (for the same type of well), the problem was separately solved in the  $CH_4$  formulation, in the form of a response function of the time of measuring the gas-air mixture state ( $t$ ) and the beginning of the working area ( $S$ ). At this stage, the definition of a maximally approximated regression for a given surface was not considered because this “transformed projection” of the regression of the response surface would have a greater approximation error than the primary surface. According to the authors’ approach, at first, the primary data were smoothed with cubic splines, and then interpolation algorithms were applied to the smoothed data, after which the final data were processed in “gnuplot”.

As a result, the obtained surfaces were projected onto the above-mentioned axes and presented graphically in Figure 4.

In Figure 4, the red rectangle shows the area (and its boundaries for two projections) of the distribution of gas flows when the local degassing network (all drainage boreholes of type no. 4 on the 18th panel) failed, and potentially recoverable methane was released into the atmosphere.

Figure 4 shows two projections of the response surface of the methane release dynamics depending on the picket number (the distance from the head to the beginning of the sublevel), the time, and the distance from the longwall. A thickened yellow line that runs parallel to the  $S$ -axis, on the  $S$ - $L$  projection and at an angle (close to 45°) shows the movement of the stopping face line at each moment of space-time on the  $S$ - $t$  projection. In addition, on the  $S$ - $t$  projection, the areas of the curves (isogases are indicated by color), outlining the projections of local maxima and minima and located below the longwall position line, determine the methane release dynamics when the longwall is still located in front of the wellhead points. Accordingly, the points of intersection between the isogases and longwall movement are the case when the longwall is still in front of the wellhead points. If the considered area, bounded by the isogas curves, is located above the longwall movement line (the upper left corner), the wellhead is located in the collapse zone (the mined-out space).

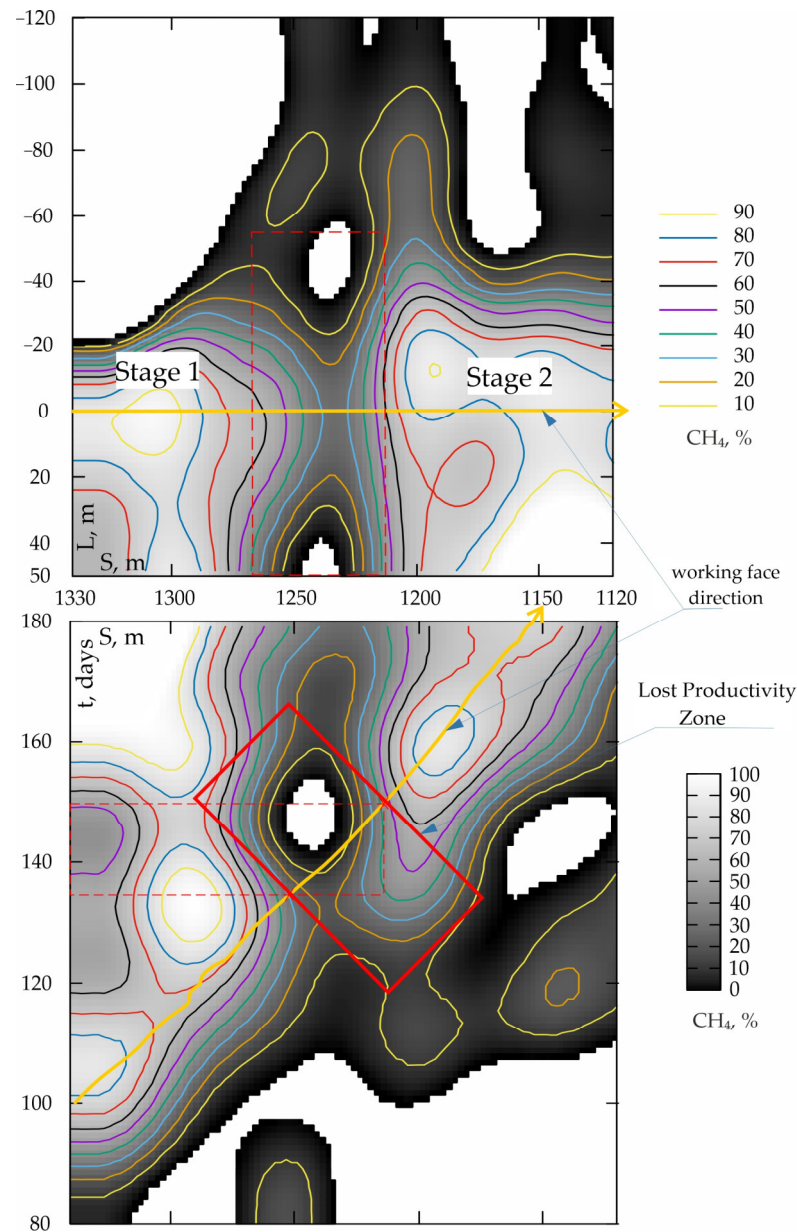


**Figure 4.** A spatial-temporal variability model of the methane concentration for all type no. 4 boreholes; S—distance from the beginning of the panel to an observation point (picket) in an air roadway of the 18th eastern panel; t—time of measurement; L—distance from a face to pickets where the boreholes are drilled;  $\text{CH}_4$ —methane content at the wellhead of each no. 4 well (picket nos. 133, 131, 128, 126, 123, 121, 119, 117, 115, 113, 111); a longwall line (marked in yellow) is a path (in space-time) that characterizes the progress of working a face relative to the beginning of a panel.

On the S-L projection, positive values along the L-axis correspond to the case when the wells are located in front of the longwall, and negative values are located behind it. Figure 1 (the S-L plane) allows the conclusion that as a result of mining coal with a high-loaded longwall, an area of conditionally minimal productivity (where the methane concentration is  $\geq 20\%$ ) is formed in the mined-out space at a distance of 20 to 35 m (S ranges from 1330 to 1280 m). After this mark (S ranges from 1280 to 1233 m), a decrease in the distance from this isogas to the straight line of longwall face movement (from 34–36 to 17 m) is observed. At the same time, a local maximum for methane release was observed 15–20 m ahead of the stopping face line (for the positive L zone) when S ranges from 1309 to 1305 m (relatively the beginning of the area) ( $\text{CH}_4 = 90\%$  denotes yellow isogas). Beyond 1300 m,



a monotonous decrease in the methane release level from 90 to 24–26% up to the mark  $S = 1233$  m is observed.

Further, (starting from the point  $S = 1233$  m) in the mined-out space, the minimum productivity area (20% is an orange curve) begins to sharply increase its linear dimensions when decreasing the distance from the sublevel beginning, reaching a maximum length of 80 m at the point  $S = 1206$  m. Then, after 1200 m, the same sharp drop in its length begins up to the level of 39–42 m in the area of the mark of 1167 m, after which it does not change until 1120 m. In the case of the area in front of the longwall, after the  $S = 1233$  m mark, a nonlinear increase up to 80% in the methane concentration in the discharged mixture containing air is observed in the area of 1160 m, accompanied by further stabilization of up to 1120 m.

Figure 4 (t-L plane) suggests that as a result of coal mining, an area of minimal gas mining productivity (20%) is formed on the 90th day from the start of mining reserves ( $S =$  from 1330 m) in the mined-out space (below the thickened yellow curve of the longwall movement). Then, until 120–124 days, its profile, which runs parallel to the longwall curve, remains stable. After that, its distance to the longwall curve begins to gradually decrease to minimum values in the range of 1250–1246 m from the beginning of the sublevel, or 132–134 days of mining reserves. At the same time, in another area, starting from 126 days (from 1220 to 1210 m before the start of the sublevel), the distance from the orange curve of 20% to the longwall line begins to increase sharply to maximum values of approximately 1212 m, after which it begins to decrease to a certain constant value. Simultaneously, ahead of the longwall, a complex pattern of forming the first local maximum can be traced in the range of 125–140 days when  $S$  varies from 1311 to 1292 m, while  $CH_4 = 90\%$ . The second zone of maximum methane extraction was in the range of 160–180 days and 1290–1330 m from the beginning of the working area. In addition to the maximum zones, the local extremum of the response surface (equal to 10 percent or less of the methane concentration) was in the range of 140–157 days and 1232–1271 m from the beginning of the working area.

We further assumed that at stage 1, methane production in all wells (on average, four wells of this type were operating simultaneously) approximately corresponded to the dynamics of picket no. 133, shown in Figure 3. For stage 2 (as can be seen from Figure 4, the area of maximum productivity for methane concentration is 20–25% more than it is at stage 1), we have 25% more methane released from the massif. To estimate degassing losses (emission fluxes) in this zone, we took the average value for the first and second stages.

The boundaries of the duration of existence of the studied zone allow us to conclude that the period of minimum degassing productivity took 15 days. After calculating the area under the methane emission flow curve (see Figure 3), the overall “L” for the conditions of the first stage  $Q$  was established to be  $6.8 \text{ m}^3/\text{min}$  for  $L \in [-40 \text{ m}; 50 \text{ m}]$ . Therefore, for stage 2,  $Q$  will be  $= 8.5 \text{ m}^3/\text{min}$  for all  $L$ , and the average productivity loss per day  $= 7.65 \text{ m}^3/\text{min}$  (or  $11,016 \text{ m}^3/\text{day}$ ). The total losses for the first no. 4 well in the “Lost Productivity Zone” are  $165,240 \text{ m}^3$ , and for all four simultaneously operating wells, they are  $660,900 \text{ m}^3$ .

#### 4. Discussion

The obtained results of the S-L projection (see the lower projection in Figure 1) indirectly confirm the ideas about the evolution of crack formation density obtained on the basis of three-dimensional modeling [63]. Proceeding from the results of this research, the authors assume that the shape of the area discharged from the stressed projection is an elliptical paraboloid. Hence, after landing the main roof (when the longwall was at the picket  $S$  in the range from 1225 to 1250 m, or from 138 to 143 days of the year), the orange curve of the isogas equal to 20% of the methane concentration probably runs parallel to the longwall line at a greater distance from it (if one draws a perpendicular down relatively to the thickened longwall line.) This means that the formed new crack system, after planting the main roof, leads to establishing more favorable conditions suitable for draining gas from the massif.

In similar cases, analytical studies on the distribution of air and gas flows are most often used [64] based on known laws of aerodynamics, and/or the actual parameters of the ventilation network are introduced into the DEM model followed by the subsequent use of CFD modeling application software packages. For example, in the conditions of the Daxing mine (Liaoning Province), namely the “Y”-type ventilation scheme, the degassing parameters of the mined-out space were modeled using FLAC3D and FLUENT software [65]. The spatial distribution of methane and leaks in the mined-out space is considered from the perspective of a porous medium model, which may not be confirmed in practice due to changes occurring in the situational geomechanical conditions in the working area. Our formation of the model of the real gas flows differs somewhat from the standard method (CFD modeling based on the continuum model). The upper projection (see Figure 1) shows the actual distribution of the methane concentration along the ventilating entry (from which the wells were drilled with a turn to the mined coal massif), which decreased in size in proportion to the growth of the mined-out space and, consequently, the main roof span (starting from  $S = 1346$  m). At the same time, it is obvious that replacing the “time— $t$ ” axis with a relative indicator of the distance from the bottom to the head of each well “ $L$ ” revealed the fact that after planting the roof, a surge (an increase in the distance from the zero thickened line) of the orange curve ( $\text{CH}_4 = 20\%$ ) in the area  $S = 1202$  m was observed. Our results confirm the presence of some inconsistencies when comparing the actual gas emission data with the model data obtained using, for example, COMSOL Multiphysics in Figure 6 of source [66]. On it, the blue dots (actual data) lie significantly higher above the red curve, based on the modeling.

Not without its limitations, but the general nature of the nonlinearities in terms of the methane concentration distribution, when the main roof span described in this research increases, is similar to the mechanism of stress changes occurring in the roof and the surrounding roof rocks, as stated in Figure 18 of source [67]. Unlike similar methods for assessing degassing productivity and volume of mine methane extraction, the authors’ method allows us to quantify gas losses due to the failure of a local degassing network. The reasons may be different, but basically it is the failure of wells associated with the peculiarities of changes in the stress–strain state in the rock mass [68–72].

The pronounced manifestations of the nonlinearity of vertical stresses, due to unequal deformations in the direction of the interlayer contacts, are shown in Figure 18c (see the radiant and purple curves). The degree of technogenic fracturing, found in the undermined rock massif, is assumed to spread unevenly, both along the massif height and in the direction of the mined-out space growth. Similarly to our studies, alternating-sign surges were observed in the methane release dynamics and the methane concentration monitored when analyzing the work on a cross-measure borehole performed at the Cheng Zhuang coal mine [68].

## 5. Conclusions

The huge volumes of mine methane overflow into the atmosphere through the mined-out space of previously abandoned horizons due to conceptual problems of underground degassing inefficiencies are conditioned by managing the roof of complete collapse.

The conducted research established the fact that when a massif was undermined as a result of mining in a full-retreat panel, reducing the distance from the beginning of the panel (increasing the roof span) from 133 to 111 pickets (220 m) in the distance range  $L$  from 50 to  $-40$  m, the methane concentration increased nonlinearly (in type 4 wells) to maximum values = 90%, which is replaced by a local minimum according to the polynomial dependence from 90 to 6%. For this reason, the emission of mine methane in the case of degasification network disruption in 15 days can amount to more than 660 thousand  $\text{m}^3$ , only for wells of type no. 4.

The authors’ technique, intended for solving spatio-temporal problems, can also be used to predict the degree of hydrocarbon vapor capture [73], or when modeling bitumen–oil mixtures [74].

**Author Contributions:** Conceptualization, V.I.G. and V.B.; methodology, E.V.V. and V.V.K.; formal analysis, V.E.G. and V.Y.K.; investigation, T.A.O.; data curation, V.E.G. and V.Y.K.; writing—original draft preparation, E.V.V. and V.V.K.; writing—review and editing, V.E.G. and V.Y.K.; supervision, V.I.G.; project administration, V.B.; visualization—T.A.O. All authors have read and agreed to the published version of the manuscript.

**Funding:** This research received no external funding.

**Institutional Review Board Statement:** Not applicable.

**Informed Consent Statement:** Not applicable.

**Data Availability Statement:** Data are contained within the article.

**Conflicts of Interest:** The authors declare no conflicts of interest.

## References

1. Silvia, F.; Talia, V.; Di Matteo, M. Coal mining and policy responses: Are externalities appropriately addressed? A meta-analysis. *Environ. Sci. Policy* **2021**, *126*, 39–47. [CrossRef]
2. Shukla, P.R.; Skea, J.; Slade, R.; Al Khouradajie, A.; van Diemen, R.; McCollum, D.; Pathak, M.; Some, S.; Vyas, P.; Fradera, R.; et al. IPCC—2022: Climate Change 2022: Mitigation of Climate Change. In *Contribution of Working Group III to the Sixth Assessment Report of the Intergovernmental Panel on Climate Change*; Cambridge University Press: Cambridge, UK, 2022; 2913p. [CrossRef]
3. Saunio, M.; Jackson, R.B.; Bousquet, P.; Poulter, B.; Canadell, J.G. The growing role of methane in anthropogenic climate change. *Environ. Res. Lett.* **2016**, *11*, 120207. [CrossRef]
4. Kopylov, A.S.; Dzhioeva, A.K.; Kondratyev, Y.I. An integrated approach to the development of the raw material base of the mining region with the use of resource-reproducing technologies. *Sustain. Dev. Mt. Territ.* **2022**, *14*, 228–239. (In Russian) [CrossRef]
5. Rybak, J.; Adigamov, A.; Kongar-Syuryun, C.; Khayrutdinov, M.; Tyulyaeva, Y. Renewable-resource technologies in mining and metallurgical enterprises providing environmental safety. *Minerals* **2021**, *11*, 1145. [CrossRef]
6. Kongar-Syuryun, C.B.; Aleksakhin, A.V.; Eliseeva, E.N.; Zhaglovskaya, A.V.; Klyuev, R.V.; Petrusevich, D.A. Modern Technologies Providing a Full Cycle of Geo-Resources Development. *Resources* **2023**, *12*, 50. [CrossRef]
7. Malyukova, L.S.; Martyushev, N.V.; Tynchenko, V.V.; Kondratiev, V.V.; Bukhtoyarov, V.V.; Konyukhov, V.Y.; Bashmur, K.A.; Panfilova, T.A. Circular Mining Wastes Management for Sustainable Production of *Camellia sinensis* (L.) O. Kuntze. *Sustainability* **2023**, *15*, 11671. [CrossRef]
8. Baumann, F.; Raga, S.R.; Lira-Cantú, M. Monitoring the stability and degradation mechanisms of perovskite solar cells by in situ and operando characterization. *APL Energy* **2023**, *1*, 011501. [CrossRef]
9. Gómez-Sanabria, A.; Kiesewetter, G.; Klimont, Z.; Schoepp, W.; Haberl, H. Potential for future reductions of global GHG and air pollutants from circular waste management systems. *Nat. Commun.* **2022**, *13*, 106. [CrossRef] [PubMed]
10. Balovtsev, S.V. Comparative assessment of aerological risks at operating coal mines. *MIAB. Min. Inf. Anal. Bull.* **2021**, *2*, 5–17. (In Russian) [CrossRef]
11. Zhanbayev, R.A.; Yerkin, A.Y.; Shutaleva, A.V.; Irfan, M.; Gabelashvili, K.; Temirbaeva, G.R.; Chazova, I.Y.; Abdykadyrkyzy, R. State asset management paradigm in the quasi-public sector and environmental sustainability: Insights from the Republic of Kazakhstan. *Front. Environ. Sci.* **2022**, *10*, 1037023. [CrossRef]
12. Godio, A.; Chiampo, F. Geophysical Monitoring of Leachate Injection in Pretreated Waste Landfill. *Appl. Sci.* **2023**, *13*, 5661. [CrossRef]
13. Balovtsev, S.V. Higher rank aerological risks in coal mines. *Min. Sci. Technol.* **2022**, *7*, 310–319. [CrossRef]
14. Zhang, K.; Liu, H.; Ma, M.; Xu, H.; Fang, H. Multiscale Fractal Characterization of Pore–Fracture Structure of Tectonically Deformed Coal Compared to Primary Undeformed Coal: Implications for CO<sub>2</sub> Geological Sequestration in Coal Seams. *Processes* **2023**, *11*, 2934. [CrossRef]
15. Brigida, V.S.; Golik, V.I.; Dmitrak, Y.V.; Gabaraev, O.Z. The impact of situational geomechanical conditions influence to improving of the drainage rock-mass caved. *Proc. Tula States Univ.-Sci. Earth* **2019**, *2*, 279–288, WOS: 000546576800026. Available online: <https://cyberleninka.ru/article/n/uchet-vliyaniya-situatsionnyh-geomehanicheskikh-usloviy-dlya-sovershenstvovaniya-degazatsii-podrabatyvaemogo-massiva-gornyh-porod> (accessed on 28 December 2023). (In Russian)
16. Efremenkov, E.A.; Martyushev, N.V.; Skeebe, V.Y.; Grechneva, M.V.; Olisov, A.V.; Ens, A.D. Research on the Possibility of Lowering the Manufacturing Accuracy of Cycloid Transmission Wheels with Intermediate Rolling Elements and a Free Cage. *Appl. Sci.* **2022**, *12*, 5. [CrossRef]
17. Klyuev, R.V.; Morgoev, I.D.; Morgoeva, A.D.; Gavrina, O.A.; Martyushev, N.V.; Efremenkov, E.A.; Mengxu, Q. Methods of Forecasting Electric Energy Consumption: A Literature Review. *Energies* **2022**, *15*, 8919. [CrossRef]
18. Golik, V.I. To the Problem of Environmental Protection of the Russian Donbass. *Mon. J. Res. Prod.* **2022**, *32*, 372022. (In Russian) [CrossRef]

19. Tian, X.; Xie, J.; Xu, M.; Wang, Y.; Liu, Y. An infinite life cycle assessment model to re-evaluate resource efficiency and environmental impacts of circular economy systems. *Waste Manag.* **2022**, *145*, 72–82. [[CrossRef](#)] [[PubMed](#)]
20. Valiev, N.G.; Golik, V.I.; Propp, V.D.; Bolgova, A.I.; Ovsyannikov, M.S. Regularities of environmental protection process management. *Min. Informational Anal. Bull.* **2022**, *11-1*, 40–50. [[CrossRef](#)]
21. Yan, J.; Xu, M. Energy and circular economy in sustainability transitions. *Resour. Conserv. Recycl.* **2021**, *169*, 105471. [[CrossRef](#)]
22. Pomili, L.; Fabrizi, F. Automotive recycling: A circular economy centre. *Environ. Eng. Manag. J.* **2020**, *19*, 1747–1753.
23. Geissdoerfer, M.; Savaget, P.; Bocken, N.M.; Hultink, E.J. The Circular Economy—A new sustainability paradigm? *J. Clean. Prod.* **2017**, *143*, 757–768. [[CrossRef](#)]
24. Kalmykova, Y.; Sadagopan, M.; Rosado, L. Circular economy—From review of theories and practices to development of implementation tools. *Resour. Conserv. Recycl.* **2018**, *135*, 190–201. [[CrossRef](#)]
25. Jia, Z.; Lin, B. How to achieve the first step of the carbon-neutrality 2060 target in China: The coal substitution perspective. *Energy* **2021**, *233*, 121179. [[CrossRef](#)]
26. Blokhin, D.I.; Zakorshmenniy, I.M.; Kubrin, S.S.; Kobylkin, A.S.; Pozdeev, E.E.; Pushilin, A.N. Numerical research of effect of stress–strain changes on stability of gas drainage wells in coal–rock mass. *Min. Informational Anal. Bull.* **2023**, *11*, 17–32. (In Russian) [[CrossRef](#)]
27. Yin, F.; Ni, X.; Han, J.; Di, J.; Zhou, Y.; Zhao, X.; Gao, Y. Impact Assessment of Hydrate Cuttings Migration and Decomposition on Annular Temperature and Pressure in Deep Water Gas Hydrate Formation Riserless Drilling. *Energies* **2023**, *16*, 5903. [[CrossRef](#)]
28. Yang, S.; Zhang, L.; Guo, J.; Huang, Y.; Xu, M. Cement production life cycle inventory dataset for China. *Resour. Conserv. Recycl.* **2023**, *197*, 107064. [[CrossRef](#)]
29. Golik, V.I.; Razorenov, Y.U.I.; Brigida, V.S.; Burdzieva, O.G. Mechanochemical technology of metal mining from enriching tails. *Bull. Tomsk. Polytech. Univ. Geo Assets Eng.* **2020**, *331*, 175–183. (In Russian) [[CrossRef](#)]
30. Shutaleva, A. Ecological Culture and Critical Thinking: Building of a Sustainable Future. *Sustainability* **2023**, *15*, 13492. [[CrossRef](#)]
31. Nepsha, F.S.; Voronin, V.A.; Liven, A.S.; Korneev, A.S. Feasibility study of using cogeneration plants at Kuzbass coal mines. *J. Min. Inst.* **2023**, *259*, 141–150. (In Russian) [[CrossRef](#)]
32. Qu, Q.; Guo, H.; Balusu, R. Methane emissions and dynamics from adjacent coal seams in a high permeability multi-seam mining environment. *Int. J. Coal Geol.* **2022**, *253*, 103969. [[CrossRef](#)]
33. Yue, G.-W.; Wang, Z.-F.; Kang, B. Prediction for isothermal adsorption curve of coal/CH<sub>4</sub> based on adsorption heat theory. *Nat. Gas Geosci.* **2015**, *26*, 148–153. [[CrossRef](#)]
34. Yang, H.-M.; Wang, Z.-F.; Ren, Z.-Y. Differences between competitive adsorption and replacement desorption of binary gases in coal and its replacement laws. *MeitanXuebao. J. China Coal Soc.* **2015**, *40*, 1550–1554. [[CrossRef](#)]
35. Li, S.; Wang, Z. Study on the Coupling Effect of Stress Field and Gas Field in Surrounding Rock of Stope and Gas Migration Law. *Energies* **2023**, *16*, 6672. [[CrossRef](#)]
36. Martyushev, N.V.; Egorov, Y.P. Determination of the signal strength with the computer analysis of the material structure. In Proceedings of the 9th International Scientific and Practical Conference of Students, Post-Graduates and Young Scientists—Modern Techniques and Technologies MTT’ 2003, Tomsk, Russia, 7–11 April 2003; pp. 192–194.
37. Khakmardan, S.; Rezaei, B.; Abdollahzadeh, A.; Ghorbani, Y. From waste to wealth: Unlocking the value of copper anode slimes through systematic characterization and pretreatment. *Miner. Eng.* **2023**, *200*, 108141. [[CrossRef](#)]
38. Brigida, V.S.; Golik, V.I.; Klyuev, R.V.; Sabirova, L.B.; Mambetalieva, A.R.; Karlina, Y.I. Efficiency Gains When Using Activated Mill Tailings in Underground Mining. *Metallurgist* **2023**, *67*, 398–408. [[CrossRef](#)]
39. Gryazev, M.V.; Kachurin, N.M.; Vorob’ev, S.A. Mathematical Models of Gas-Dynamic and Thermophysical Processes in Underground Coal Mining at Different Stages of Mine Development. *J. Min. Inst.* **2017**, *223*, 99–108. (In Russian) [[CrossRef](#)]
40. Campo, G.; Ruffino, B.; Reyes, A.; Zanetti, M. Water-Energy Nexus in the Antofagasta Mining District: Options for Municipal Wastewater Reuse from a Nearly Energy-Neutral WWTP. *Water* **2023**, *15*, 1221. [[CrossRef](#)]
41. Slastunov, S.; Kolikov, K.; Batugin, A.; Sadov, A.; Khautiev, A. Improvement of Intensive In-Seam Gas Drainage Technology at Kirova Mine in Kuznetsk Coal Basin. *Energies* **2022**, *15*, 1047. [[CrossRef](#)]
42. Zhao, C.; Cheng, Y.; Li, W.; Zhang, K.; Wang, C. Critical stress related to coalbed methane migration pattern: Model development and experimental validation. *Energy* **2023**, *284*, 128681. [[CrossRef](#)]
43. Hosseini, A.; Najafi, M.; Hossein Morshedy, A. Determination of suitable distance between methane drainage stations in Tabas mechanized coal mine (Iran) based on theoretical calculations and field investigation. *J. Min. Inst.* **2022**, *258*, 1050–1060. [[CrossRef](#)]
44. Li, Y.; Wu, S.; Nie, B.; Ma, Y. A new pattern of underground space-time Tridimensional gas drainage: A case study in Yuwu coal mine, China. *Energy Sci. Eng.* **2019**, *7*, 399–410. [[CrossRef](#)]
45. Jiangfu, H.; Wenchao, H.; Chengpeng, Z.; Zhongguang, S.; Xiaoyi, S. Numerical simulation on the deformation characteristics of borehole failure in gas-bearing coal seams considering the effective stress principle under complicated stress path conditions. *Geomech. Geophys. Geo Energy Geo Resour.* **2022**, *8*, 95. [[CrossRef](#)]
46. Xiang, Y.; Lan, J.; Cai, Y.; Dong, Y.; Hou, H. Preparation of nickel–cobalt tailings-based cementing materials by mechano-chemical activation: Performance and mechanism. *Constr. Build. Mater.* **2023**, *408*, 133836. [[CrossRef](#)]

47. Qu, Q.; Shi, J.; Wilkins, A. A Numerical Evaluation of Coal Seam Permeability Derived from Borehole Gas Flow Rate. *Energies* **2022**, *15*, 3828. [[CrossRef](#)]
48. Zhao, P.; An, X.; Li, S.; Kang, X.; Huang, Y.; Yang, J.; Jin, S. Study on the Pseudo-Slope Length Effect of Buried Pipe Extraction in Fully Mechanized Caving Area on Gas Migration Law in Goaf. *Sustainability* **2023**, *15*, 6628. [[CrossRef](#)]
49. Gorelkina, E.I.; Mugisho, J.B.; Kouadio, K.S. Waterflooding, water-gas method and generation of carbon dioxide in the reservoir—Methods of enhanced oil recovery and technology development. In *IOP Conference Series: Earth and Environmental Science*; IOP: Bristol, UK, 2023; Volume 1212, p. 012038. [[CrossRef](#)]
50. Montano, J.; Coco, G.; Antolinez, J.A.A.; Beuzen, T.; Bryan, K.R.; Cagigal, L.; Castelle, B.; Davidson, M.A.; Goldstein, E.B.; Ibace-ta, R.; et al. Blind testing of shoreline evolution models. *Sci. Rep.* **2020**, *10*, 2137. [[CrossRef](#)]
51. Chicco, D.; Warrens, M.J.; Jurman, G. The coefficient of determination R-squared is more informative than SMAPE, MAE, MAPE, MSE and RMSE in regression analysis evaluation. *PeerJ Comput. Sci.* **2021**, *7*, e623. [[CrossRef](#)] [[PubMed](#)]
52. Brigida, V.S.; Zinchenko, N.N. Methane Release in Drainage Holes Ahead of Coal Face. *J. Min. Sci.* **2014**, *50*, 60–64. [[CrossRef](#)]
53. Pan, H.-Y.; He, S.-N.; Zhang, T.-J.; Song, S.; Wang, K. Application of an improved naive Bayesian analysis for the identification of air leaks in bore-holes in coal mines. *Sci. Rep.* **2022**, *12*, 16081. [[CrossRef](#)]
54. Mayet, A.M.; Gorelkina, E.I.; Fouladinia, F.; Sh Daoud, M.; Thafasaljyas, V.P.; Kumar Shukla, N.; Sayeeduddin Habeeb, M.; HALhashim, H. An artificial neural network and a combined capacitive sensor for measuring the void fraction in-dependent of temperature and pressure changes for a two-phase homogeneous fluid. *Flow Meas. Instrum.* **2023**, *93*, 102406. [[CrossRef](#)]
55. Haque, I.; Siam Abdullah, M.; Khairul Islam, M.; Enamullah, M. Synthesis, PXRD structure, spectroscopy, cyclic voltammogram, thermal analysis and DFT/TD-DFT calculations of bis[*salicylaldehydato-κO,O'*]nickel(II). *Inorganica Chim. Acta* **2023**, *550*, 121430. [[CrossRef](#)]
56. Dmitriev, A.N.; Vyaznikova, E.A.; Vitkina, G.Y.; Karlina, A.I. A Study of the Structure and Physicochemical Properties of the Mixed Basicity Iron Ore Sinter. *Magnetochemistry* **2023**, *9*, 212. [[CrossRef](#)]
57. Isametova, M.E.; Martyushev, N.V.; Karlina, Y.I.; Kononenko, R.V.; Skeeba, V.Y.; Absadykov, B.N. Thermal Pulse Processing of Blanks of Small-Sized Parts Made of Beryllium Bronze and 29 NK Alloy. *Materials* **2022**, *15*, 6682. [[CrossRef](#)] [[PubMed](#)]
58. Bosikov, I.I.; Martyushev, N.V.; Klyuev, R.V.; Savchenko, I.A.; Kukartsev, V.V.; Kukartsev, V.A.; Tynchenko, Y.A. Modeling and Complex Analysis of the Topology Parameters of Ventilation Networks When Ensuring Fire Safety While Developing Coal and Gas Deposits. *Fire* **2023**, *6*, 95. [[CrossRef](#)]
59. Brigida, V.S.; Golik, V.I.; Dmitrak, Y.V.; Gabaraev, O.Z. Ensuring stability of undermining inclined drainage holes during intensive development of multiple gas-bearing coal layers. *J. Min. Inst.* **2019**, *239*, 497–501. [[CrossRef](#)]
60. Abdullah, G.M.S.; Abd El Aal, A.; Al Saiari, M.; Radwan, A.E. Sustainable Impact of Coarse Aggregate Crushing Waste (CACW) in Decreasing Carbon Footprint and Enhancing Geotechnical Properties of Silty Sand Soil. *Appl. Sci.* **2023**, *13*, 10930. [[CrossRef](#)]
61. Kondrakhin, V.P.; Martyushev, N.V.; Klyuev, R.V.; Sorokova, S.N.; Efremenkov, E.A.; Valuev, D.V.; Mengxu, Q. Mathematical Modeling and Multi-Criteria Optimization of Design Parameters for the Gyrotory Crusher. *Mathematics* **2023**, *11*, 2345. [[CrossRef](#)]
62. Malozyomov, B.V.; Golik, V.I.; Brigida, V.; Kukartsev, V.V.; Tynchenko, Y.A.; Boyko, A.A.; Tynchenko, S.V. Substantiation of Drilling Parameters for Undermined Drainage Boreholes for Increasing Methane Production from Unconventional Coal-Gas Collectors. *Energies* **2023**, *16*, 4276. [[CrossRef](#)]
63. Chen, J.; Zhou, L.; Xia, B.; Su, X.; Shen, Z. Numerical Investigation of 3D Distribution of Mining-Induced Fractures in Response to Longwall Mining. *Nat. Resour. Res.* **2021**, *30*, 889–916. [[CrossRef](#)]
64. Chen, Y.; Liu, R.; Xuan, P. A calculation method of gas emission zone in a coal mine considering main controlling factors. *Sci. Rep.* **2021**, *11*, 23597. [[CrossRef](#)]
65. Zhou, X.; Jing, Z.; Li, Y. Research on controlling gas overrun in a working face based on gob-side entry retaining by utilizing ventilation type “Y”. *Sci. Rep.* **2023**, *13*, 9199. [[CrossRef](#)]
66. Xia Tq Xu, M.j.; Wang, Y.I. Simulation investigation on flow behavior of gob gas by applying a newly developed FE software. *Environ. Earth Sci.* **2017**, *76*, 485. [[CrossRef](#)]
67. Wang, Q.; Wang, Y.; He, M.; Li, S.; Jiang, Z.; Jiang, B.; Xu, S.; Wei, H. Experimental study on the mechanism of pressure releasing control in deep coal mine roadways located in faulted zone. *Geomech. Geophys. Geoenerg. Georesour.* **2022**, *8*, 50. [[CrossRef](#)]
68. Zhang, B.; Liang, Y.; Sun, H.; Wang, K.; Zou, Q.; Dai, J. Evolution of mining-induced fractured zone height above a mined panel in longwall coal mining. *Arab. J. Geosci.* **2022**, *15*, 476. [[CrossRef](#)]
69. Zakharov, V.N.; Shlyapin, A.V.; Trofimov, V.A.; Filippov, Y.A. Change in stress-strain behavior of coal-rock mass during coal mining. *Min. Informational Anal. Bull.* **2020**, *79*, 5–24. (In Russian) [[CrossRef](#)]
70. Xu, J.; Li, H.; Wang, H.; Tang, L. Experimental study on 3D internal penny-shaped crack propagation in brittle materials under uniaxial compression. *Deep Undergr. Sci. Eng.* **2023**, *2*, 37–51. [[CrossRef](#)]
71. Demenkov, P.A.; Romanova, E.L.; Kotikov, D.A. Stress–strain analysis of vertical shaft lining and adjacent rock mass under conditions of irregular contour/MIAB. In *Mining Informational and Analytical Bulletin*; Saint Petersburg Mining University: Saint Petersburg, Russia, 2023; pp. 33–48.
72. Wei, H.; Wu, H.; Ren, G.; Tang, L.; Feng, K. Energy-based analysis of seismic damage mechanism of multi-anchor piles in tunnel crossing landslide area. *Deep Undergr. Sci. Eng.* **2023**, *2*, 245–261. [[CrossRef](#)]

73. Zakirova, G.; Pshenin, V.; Tashbulatov, R.; Rozanova, L. Modern Bitumen Oil Mixture Models in Ashalchinsky Field with Low-Viscosity Solvent at Various Temperatures and Solvent Concentrations. *Energies* **2023**, *16*, 395. [[CrossRef](#)]
74. Korshak, A.A.; Nikolaeva, A.V.; Nagatkina, A.S.; Gaysin, M.T.; Korshak, A.A.; Pshenin, V.V. Method for predicting the degree of hydrocarbon vapor recovery at absorption. *Sci. Technol. Oil Oil Prod. Pipeline Transp.* **2020**, *10*, 202–209. [[CrossRef](#)]

**Disclaimer/Publisher’s Note:** The statements, opinions and data contained in all publications are solely those of the individual author(s) and contributor(s) and not of MDPI and/or the editor(s). MDPI and/or the editor(s) disclaim responsibility for any injury to people or property resulting from any ideas, methods, instructions or products referred to in the content.